Proceedings of the Thirty-fourth (2024) International Ocean and Polar Engineering Conference **www.isope.org**
Rhodes, Greece, June 16–21, 2024

ISBN 978-1-880653-78-4; ISSN 1098-6189

Numerical Study of Internal Waves Induced by a Moving Submarine Model in Two-Layer Fluids

Linjie Li[1], Qingjie Meng[2], Liushuai Cao[1], Decheng Wan[1]*

[1] Computational Marine Hydrodynamics Lab (CMHL), School of Naval Architecture, Ocean and Civil Engineering,
Shanghai Jiao Tong University, Shanghai, China
[2] Wuhan Second Ship Design and Research Institute, Wuhan, China

[*]Corresponding Author

ABSTRACT

The actual marine environment forms a density stratified environment in the vertical direction, the motion of a submarine and other underwater vehicles will form free surface waves as well as internal waves in a stratified fluid. The impact of free surface fluctuation on internal waves varies as the submarine moves at different cruising speeds. In order to investigate this problem, this paper first qualitatively analyzes the waveform results of internal waves when a submarine model moves at different speeds preserving the free-surface and using the rigid lid assumption respectively, and then quantitatively calculates the internal wave results when the submarine model moves at various cruising speeds based on numerical simulation. The results indicate that if the velocity of the submarine is small, the waveform results of internal waves with both the free surface and the rigid lid approximation are only V-shaped waves. However, when the submarine moves at the maximum cruising speed, in addition to divergent waves, transverse waves emerge in the waveform of internal waves. A comparison with results obtained under the condition of rigid lid reveals that these transverse waves are caused by corresponding disturbances of the free surface.

KEY WORDS: Density stratification; internal wave; divergent wave; transverse wave; rigid lid assumption.

INTRODUCTION

In the actual ocean, due to the influence of temperature difference, salinity and other factors, the brine will have the phenomenon of density stratification (Zhang et al. 2006, Mao and Zhang, 2013). When underwater objects move in the stratified liquid, they will form wakes with specific shapes on interfaces. The position of moving objects can be predicted by detecting the wake features. At different cruising speeds, free surface waves stimulated by object motion will also affect the characteristic of internal wave shapes to different degrees. Therefore, it is of great academic significance and practical application value to study the free surface effect on internal waves excited by a submarine.

Theoretical research in two-layer fluids began early. Grue et al. (1997) studied the problem of large internal solitary waves excited by a two-dimensional semi-elliptic object moving in the seafloor under the rigid lid. Yeung and Nuyen (1999) proposed that in two layers of fluid with a finite depth, waves generated by a moving point source have free surface wave mode and internal wave mode. Wei et al. (2003) studied the influence of internal waves generated by the moving point source in the lower fluid on the free surface waves, the results showed that the free surface divergence field induced by internal wave mode is equivalent to the contribution of surface wave mode, and the two have a strong coupling effect. Zhao et al. (2020) studied the propagation of internal solitary waves when there is no object between two layers fluid, and found that when the density ratio between two constant density fluids is close to 1, the rigid lid assumption is reasonable, for large density differences, the free surface effect must be considered. These theoretical derivations are very efficient and instructive, but there are still great differences between these ideal models and the submarine model with complex shape and structure in practice.

With the advent of computational power and numerical algorithms, researchers began to perform numerical simulations in stratified fluids. Based on the experiment of Arntsen (1996), Ma et al. (2016) simulated the change characteristics of internal wave height and wavelength induced by a cylinder moving under different depth and density Froude number. Zhang et al. (2022) simulated the internal wave propagation process generated by plate flapping in the two layers fluid under two surface boundary conditions based on Fluent, and found that the change of density difference did not significantly affect the consistency between theoretical and numerical solutions. Wang et al. (2022) studied the motion response of submarine after encountering internal solitary waves under the rigid hypothesis.

From the current research status, the numerical studies have not discussed the influence of free surface waves induced by a submarine model moving at typical cruising speed on internal waves. And this is the motivation of this paper.

The remaining content of this paper is structured as follows: Section two introduces the numerical calculation model, followed by Section three presenting the results and discussions, and finally, Section four provides a concise summary.

NUMERICAL CALCULATION MODEL

Governing Equation

The fluid is assumed as viscous and incompressible. The mass and momentum conservation equation (i.e. the Navier-Stokes equation) for the flow mass points in STAR-CCM + solution is as Eqs. 1~2 (Ferziger et al. 1997).

$$\frac{\partial \rho}{\partial t}+\nabla\cdot\rho\,\boldsymbol{v}=0 \tag{1}$$

$$\rho\frac{D\boldsymbol{v}}{Dt}=\rho g-\nabla p+\mu\nabla^2\boldsymbol{v} \tag{2}$$

Where ρ represents the fluid density within each layer, $\boldsymbol{v}$ denotes the velocity of the fluid particle, p signifies the pressure, and g = 9.8 m/s^2 corresponds to the gravitational acceleration. The Reynolds-averaged Navier-Stokes (RANS) equation can be derived from a time-averaged Navier-Stokes equation, and subsequently solved using the realizable k–ε turbulence model in STAR-CCM+.

The VOF Method

The free surface waves and internal waves can be accurately tracked and resolved using the volume of fluid (VOF) method, which effectively addresses interface problems by computing the volume fraction of each phase within every grid. The VOF technique is widely employed in contemporary finite volume methods (Gopala and Van Wachem, 2008). Assuming $r^{(k)}$ represents the proportion of the k^{th} phase in a cellular grid based on the principle of mass conservation, it can derive Eq.3.

$$\sum_{k=1}^{n} r^{(k)}=1 \tag{3}$$

The volume fraction $r^{(k)}$ can be calculated from dividing the volume of each phase by the total volume, as Eq.4.

$$r^{(k)}=\frac{V^{(k)}}{\sum_{k=1}^{n}V^{(k)}} \tag{4}$$

In this paper, if the free surface is preserved, three distinct phases will coexist: air, fresh water, and sea water. Therefore, n = 3, k = 1, 2, and 3. However, if the rigid lid assumption is employed instead of the free surface condition, only two phases will be present, which is fresh water and sea water. The fluctuations of internal waves can be accurately determined by monitoring the vertical position of an iso-surface with a volume fraction of sea water set at 50%.

Boundary Conditions

This paper focuses on investigating internal waves of the SUBOFF fully appended submarine in a two-layer stratified liquid. The upper fluid layer, denoted as h_1, is characterized by a small thickness and has a density of ρ_1. The lower fluid layer, denoted as h_2, possesses a larger thickness and is characterized by a density of ρ_2. The submarine exhibits steady motion at various cruising speeds, which induces disturbances on the free surface and internal surface resulting in waves formation.

Because the submarine model is eudipleural, the longitudinal section of the submarine is designated as a symmetrical boundary. The surface of the submarine is set as non-slip wall, while the inlet and bottom are assigned velocity inlet boundary conditions. The outlet is set as pressure outlet boundary condition, and the side of the calculation domain are defined as symmetric boundary. When considering the free surface, the top is subjected to velocity inlet boundary condition; however, when utilizing rigid lid assumption, it assumes a symmetric boundary condition at the top, as shown in Figure 1.

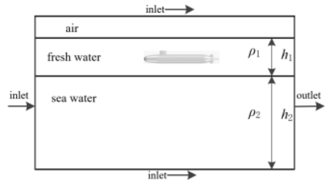

(a) Preserving free surface

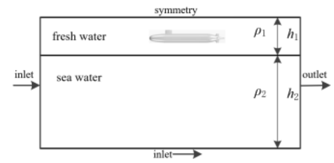

(b) Rigid lid condition

Fig. 1 Schematic of the boundary condition configuration

The Euler multiphase flow model is utilized to define the densities of fresh water and sea water. Additionally, the user-defined field function module sets the initial distribution of each phase and pressure function.

Computational Domain and Mesh

The SUBOFF fully appended submarine model employed in this paper is a standardized submarine model specifically developed by the Defense Advanced Research Projects Agency (DARPA) of the United States to provide reliable comparative data for numerical simulation results. The geometric representation of this model can be observed in Figure 2, while Table 1 presents the key parameters of the SUBOFF submarine model.

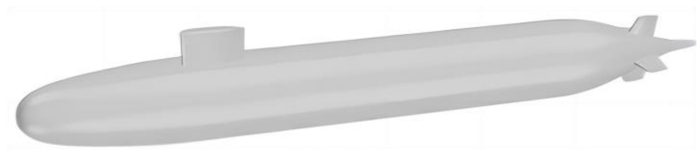

Fig. 2 The SUBOFF fully appended submarine model

Table 1. Main parameters of the SUBOFF model

Parameters	Symbol	Value
Overall length	L_{OA} (m)	4.356
Maximum diameter	D_{max} (m)	0.508
Center of buoyancy position	X_B (m)	2.013
Wet surface area	$S_{\omega A}$ (m^2)	5.989
Displacement	∇ (m^3)	0.699

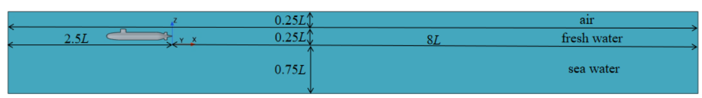

(a) Front view for preserving free surface

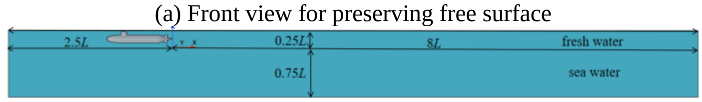

(b) Front view for rigid lid condition

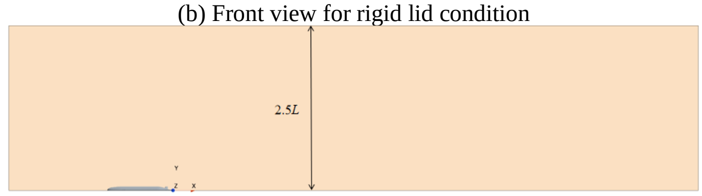

(c) Top view

Fig. 3 Size of the computational domain

The entire calculation domain is a rectangular region with the coordinate origin located on the inner interface. The length of the calculation domain measures 10.5 L, while its width and height are 2.5 L and 1 L respectively. The upstream size is set at 2.5 L, whereas the downstream size is set at 8 L. The distance between the internal surface and the bottom of the calculation domain amounts to 0.75 L, while the distance

between the free surface and the internal surface equals 0.25 L.
If the free surface flow is taken into account, corresponds to the condition of preserving free surface, an additional layer of air with a height equivalent to 0.25 L is incorporated at the upper part of the free surface. When the rigid lid assumption is used, there would be no air. The size diagram of the calculation domain is shown in Figure 3.
The computing domain is divided using STAR-CCM+ trimmed volume mesh and boundary layer mesh generator. In addition to the overall meshing of the entire computing domain, specific attention is given to refine the grid near the SUBOFF model and relevant areas from the free surface to the internal surface. The size of mesh refinement in this region varies based on different working conditions, ensuring appropriate resolution for wave amplitudes. To ensure smooth transitions, both surface and volume mesh growth rates are set to slow. Figure 4 illustrates grid refinement on the surface of the SUBOFF submarine model as well as the correlation region within the calculation domain.

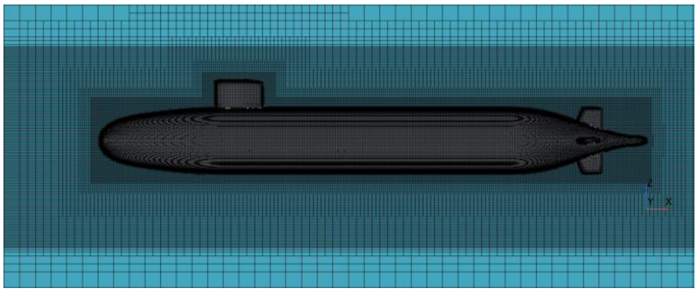

Fig. 4 Mesh section of computational domain

For the problem of internal wave excitation in the density stratified fluid by a submarine with steady motion, the numerical verification results have already been accomplished in prior research (li et al. 2023) and will not be reiterated herein.

RESULTS AND DISCUSSIONS

Firstly, the application of linear theory is employed to qualitatively analyze the waveform of internal waves stimulated by submarine motion at various speeds in the presence of free-surface. Subsequently, numerical simulations using STAR-CCM+ are conducted under three representative speed conditions, and a comparative analysis is performed between the theoretical findings and numerical results. Furthermore, both theoretical analysis and numerical simulation are carried out considering the rigid cover hypothesis. Finally, the influence of free surface effect on the internal wave form is analyzed and summarized.

The Internal Waves under the Condition of Preserving Free Surface

Based on the Landau and Lifshitz (1959), Faltinsen (2006) conducted a qualitative analysis of the internal surface waveform generated by an object moving at various velocities under the circumstance of two-layer fluid system and had taken the free surface into account. He proposed that when the free surface is preserved, the density Froude number can be defined as Eq. 5.

$$F_{FS}^2 = \frac{U^2}{g\dfrac{\rho_2 - \rho_1}{\rho_2}h_1} \tag{1}$$

F_{FS}=1 is the critical Froude density number. If F_{FS}<1, that is, when the velocity of the object is less than the critical Froude density number, transverse (perpendicular to the trajectory direction of the object) wave and the V-shaped divergent wave can appear on the internal surface. If F_{FS}>1, that is, when the velocity of the object is greater than the critical Froude number of density, only divergent wave can be observed on the internal surface.
The fluid densities of the upper and lower layer are 1000 kg/m^{3}and 1020 kg/m^3 respectively in this paper. Because the submarine's actual cruising speed ranges from 4 to 30 kn, the present work focuses on three representative speed conditions and the corresponding model working conditions in Table 2.
According to the conclusion of Faltinsen, the F_{FS} values in the three cases exceed 1, indicating that only divergent waves should be observed on the internal surface.

Table 2. Cases of three typical cruising speeds for free surface boundary

Case number	1	2	3
SUBOFF	Speed		
Actual scale (87.12 m)	4 kn	15 kn	30 kn
Model scale (4.356 m)	0.460 m/s	1.725 m/s	3.451m/s
F_{FS}	1.01	3.77	7.54

Within a fixed calculation domain, the internal wave results induced by the motion of SUBOFF fully appended submarine model under different cruising speeds will not change after a certain period of time. Figure 5 shows the final situation of the internal surface fluctuations induced by the motion of the submarine model under three typical cruising speeds. In order to facilitate a more intuitive comparison of fluctuations across various cruising speeds, consistent intervals have been maintained in post-processing for scalar fields.

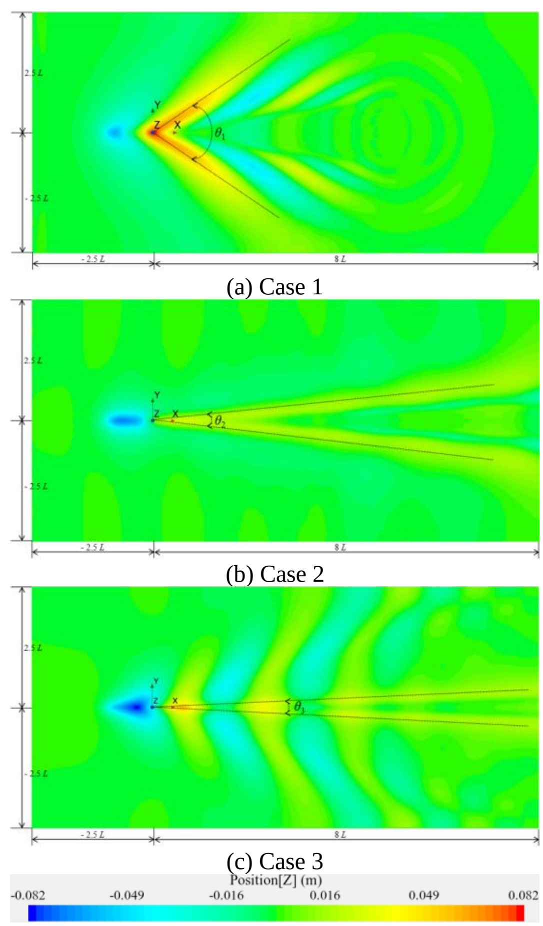

Fig. 5 Top view of the internal surface for preserving free surface

From Figure 5, it is evident that the internal surface waveforms induced by the submarine model movement at the three typical cruising speeds exhibit V-shaped divergent waves, which aligns with theoretical derivation. As denoted in the figure that $\theta_1 = 66^\circ$, $\theta_2 = 13^\circ$, and $\theta_3 = 6^\circ$, the angle of the V-shaped divergent waves decreases with the velocity increases. However, it is noteworthy that when the submarine model operates at its maximum cruising speed (equivalent to 30 kn of a real-scale submarine), not only divergent waves but also transverse waves appear on the internal surface. These two wave systems together form the characteristic shape similar to Kelvin wave.

The Kelvin waveform is common in free surface waves. This section preserves the free surface, so the free surface wave results can also be obtained, as shown in Figure 6. It should be noted that the coordinate system is set as shown in Figure 3, and the origin point is set to the equilibrium position of the inner interface. The X-axis denotes positivity when directed towards the submarine tail, while positivity along the Y-axis indicates direction towards one side of the calculation domain. Similarly, upward direction along Z-axis signifies positivity. Consequently, Z_0=0.25 L represents the equilibrium position of the free surface.

As can be seen from Figure 6, when the submarine is moving at the lowest cruising speed, there is almost no fluctuation on the free surface. When the cruising speed is medium, the free surface fluctuation is very small. Only when the submarine is moving at the maximum cruising speed can large fluctuations be seen on the still water surface, and the transverse wave system of the free plane corresponds to that of the internal surface.

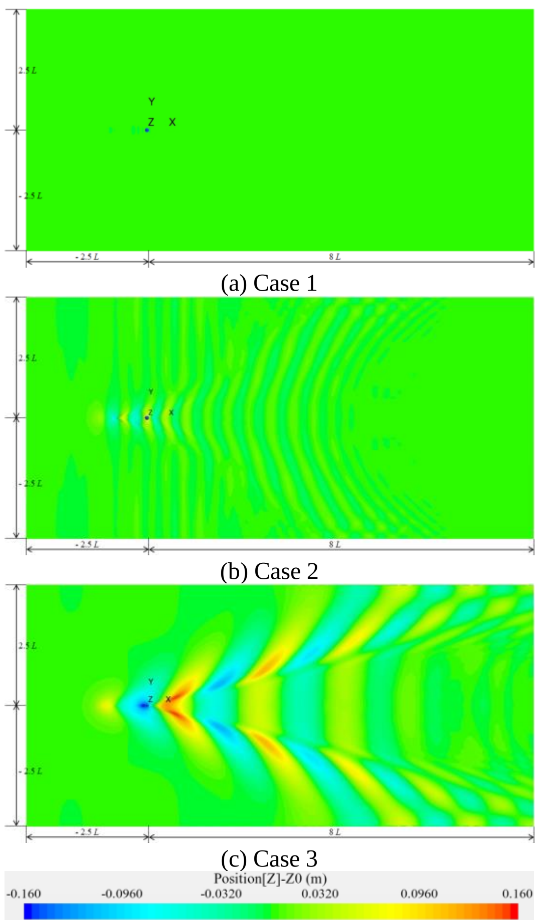

(a) Case 1

(b) Case 2

(c) Case 3

Fig. 6 Top view of the free surface at three typical cruising speeds

So as to verify whether the transverse waves on the free surface are responsible for the transverse waves observed on the internal surface, it is imperative to investigate the waveform results of the internal surface under the condition of rigid lid.

The Internal Waves under the Condition of Rigid Lid

Before commencing the numerical computation, it is advisable to conduct a qualitative analysis of the waveform outcomes pertaining to the internal surface through a concise linear theoretical derivation.

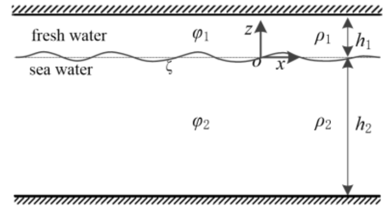

Fig. 7 Internal waves under the rigid lid condition

For the problem of two layers of fluid under the rigid lid condition in a finite water depth, as shown in Figure 7, Landau and Lifshitz (1959) provide the dispersion relationship of the internal surface as depicted in Eq. 6.

$$\frac{\omega^2}{gk} = \frac{\rho_2 - \rho_1}{\rho_1 cth(kh_1) + \rho_2 cth(kh_2)} \quad (2)$$

But Landau and Lifshitz did not take the motion of a subject into account. The relationship between the coordinate system fixed with the moving object and the earth coordinate system is shown in Figure 8.

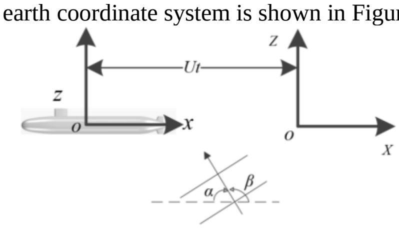
Fig. 8 The relation between the moving and earth coordinates

The relation between the two coordinate systems is Eq. 7.

$$\mathrm{x} = \mathrm{X} + \mathrm{Ut}, \mathrm{y} = \mathrm{Y}, \mathrm{z} = \mathrm{Z} \quad (3)$$

A regular wave with amplitude ζ_a and angle β propagating relative to the X-axis can be expressed as Eq. 8 in the geodetic coordinate system.

$$\zeta = \zeta_a \cos(kXcos\beta + kYsin\beta - \omega t - \epsilon) \quad (4)$$

Convert to the coordinate system fixed with the moving object, and get Eq. 9.

$$\zeta=\zeta_a\cos(kx\cos\beta+ky\sin\beta-(kUcos\alpha-\omega)t-\epsilon) \quad (5)$$

Since the internal interface waves observed in the coordinate system fixed with the moving object are independent of time, it is required Eq. 10.

$$kUcos\alpha = \omega \quad (6)$$

So it can get the relation as Eq. 11.

$$\frac{\omega^2}{gk} = \frac{\rho_2 - \rho_1}{\rho_1 cth(kh_1) + \rho_2 cth(kh_2)} = \frac{kU^2cos^2\alpha}{g} \quad (7)$$

The density Froude number under rigid lid boundary condition can be defined as Eq. 12.

$$F_{RL}^2 = \frac{U^2}{g\frac{\rho_2 - \rho_1}{\rho_2}\frac{h_1 h_2}{h_1 + h_2}} \quad (8)$$

Then the Eq. 13 can be obtained as:

$$F_{RL}^2(\cos\alpha)^2\left(k\frac{h_1h_2}{h_1+h_2}\right)\left(\frac{\rho_2-\rho_1}{\rho_2}\right)=\frac{\rho_2-\rho_1}{\rho_1 cth(kh_1)+\rho_2 cth(kh_2)} \quad (9)$$

In a specific case, the lower water depth h_2 can be expressed as nh_1 by the upper water depth h_1, so the above Eq. 13 becomes Eq. 14:

$$F_{RL}^2(\cos\alpha)^2(kh_1)=\frac{\rho_2}{\rho_1 cth(kh_1)+\rho_2 cth(nkh_1)}\left(\frac{1+n}{n}\right) \quad (10)$$

Defining a function $f_1(\mathrm{x})=\frac{\rho_2}{\rho_1 cth(x)+\rho_2 cth(nx)}\left(\frac{1+n}{n}\right)$, it can geometrically find the intersection of the line y=$F_{RL}^2(\cos\alpha)^2x$and the curve $f_1(x)$. By substituting the environmental specific parameters ρ_1、ρ_2、h_1、h_2 into $f_1(x)$, it can obtain $\lim_{\Delta x\to 0}\frac{f_1(0+\Delta x)-f_1(0)}{\Delta x}=1$, therefore, when $F_{RL}^2(\cos\alpha)^2$<1, the line y=$F_{RL}^2(\cos\alpha)^2x$ intersects with curve $f_1(x)$, as shown in the Figure 9.

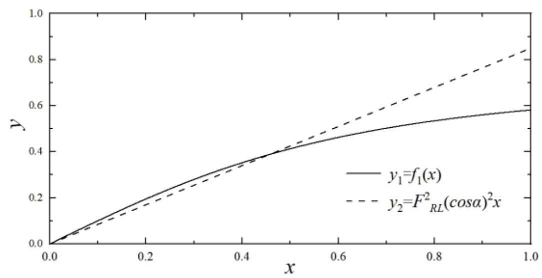

Fig. 9 Diagram of intersection between curve $f_1(x)$ and line y=$F_{RL}^2(\cos\alpha)^2x$

Therefore, F_{RL}=1 is the critical Froude number of the density, if F_{RL}<1, then for all α, there is a solution, that is, when the velocity of the object is less than the critica Froude number of the density, the transverse wave and divergent wave can appear on the internal surface. If F_{RL}>1, then there is no solution of α=0 (corresponding to the transverse wave), and $|\alpha_{min}|=\cos^{-1}(1/F_{RL})$ (corresponding to the divergent wave), that is, when the velocity of the object is greater than the critical Froude number of density, only divergent waves can appear on the internal surface.

The F_{RL} corresponding to the three speeds are presented in Table 3, because the values of the F_{RL} are all greater than 1, according to linear theory analysis, only divergent waves should be observed on the internal surface for these three cases.

Table 3. Cases of three typical cruising speeds for rigid lid condition

Case number	4	5	6
SUBOFF	Speed		
Actual scale (87.12 m)	4 kn	15 kn	30 kn
Model scale (4.356 m)	0.460 m/s	1.725 m/s	3.451m/s
F_{RL}	1.16	4.35	8.70

Figure 10 shows the internal waves induced by the motion of a submarine model at three typical cruising speeds under the condition of rigid lid. For the purpose of facilitating an intuitive comparison with Figure 5, the scalar field has been adjusted to align with the same interval.

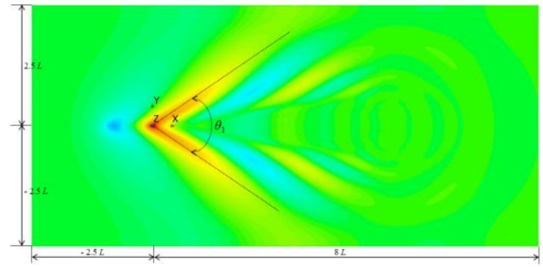

(a) Case 4

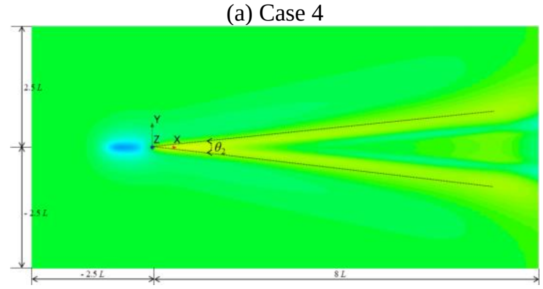

(b) Case 5

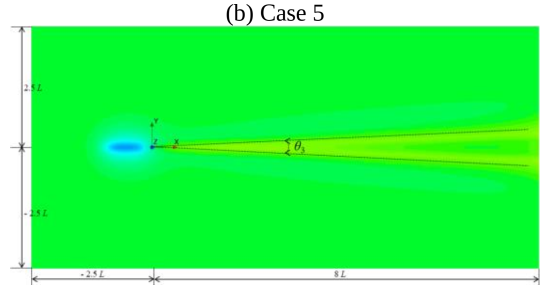

(c) Case 6

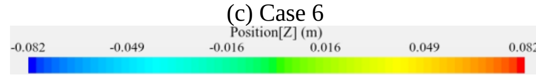

Fig. 10 Top view of the internal surface for rigid lid condition

As depicted in Figure 10, under the boundary condition of the rigid lid, the internal waves stimulated by the submarine model moving at three typical cruising speeds have only V-shaped divergent waves. The theoretical analysis aligns with the numerical results.

In addition, by comparing Figure 5 (c) with Figure 10 (c), it can be clearly concluded that transverse waves on internal surface are influenced by the free surface wave system at the maximum cruising speed. This conclusion can be further proved by the vertical velocity field of the internal surface, as shown in Figure 11.

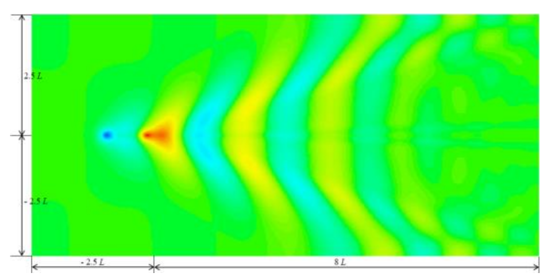

(a) Preserving free surface

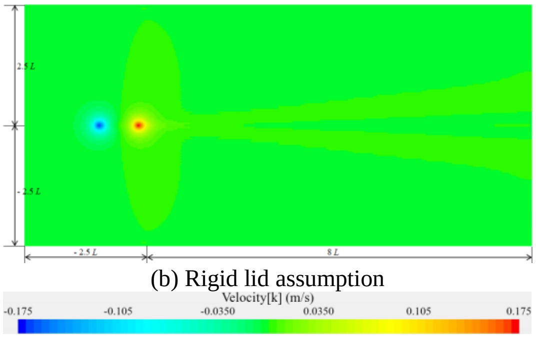

(b) Rigid lid assumption

Fig. 11 The vertical velocity field of the internal surface

In order to quantitatively study the influence of free surface on internal waves maximum amplitude, the results of the maximum fluctuation of internal surface under the two conditions are summarized as Table 4 respectively.

Table 4. Internal surface maximum fluctuation amplitude for all cases

Speed/(m/s)		0.460	1.725	3.451
Amplitude/m	FS	0.1436	0.09590	0.3364
	RL	0.1434	0.09476	0.1361
Relative value/%	A_{FS}/A_{RL}	100.1	101.2	247.2

As can be seen from Table 4, when the speed of the submarine model is less than 1.725m/s (corresponding to 15 kn of an actual scale), the amplitude difference of the internal surface under the two conditions is within 1.2%. Only when the submarine moves at the maximum cruising speed, the amplitude of the preserving free surface condition is 247.2% of the amplitude under the rigid lid assumption.

CONCLUSIONS

In this paper, the internal waves stimulated by a submarine model moving at different cruising speeds for preserving free surface and rigid lid assumption respectively are investigated. Firstly, the waveform of internal surface are qualitatively analyzed by linear theory, and then quantitatively calculated by STAR-CCM+. The main conclusions are as follows:

(1) For the problem of two layers fluid in a finite depth, the critical Froude number corresponding to the velocity can be determined through analysis of linear theory, regardless of whether the free surface is retained or the rigid lid is applied, when the Froude number exceeds this critical value, only divergent waves can be observed on the internal surface, otherwise, both transverse waves and divergent waves can be observed.

(2) For the cases considered in the present work, when corresponding cruising speed of the submarine is low, such as 4 kn and 15 kn, only V-shaped divergent waves are observed on the internal surface. The theoretical analysis aligns well with the numerical results. It is noteworthy that the free surface waves exert little effect on internal waves.

(3) In the working condition of this paper, when the submarine moves at the maximum cruising speed, the fluctuation on the free surface will affect the internal surface downward. At this time, rigid lid cannot be used to replace the free surface, otherwise the transverse waves cannot be seen on the internal surface, and the amplitude of the internal waves will be reduced to the original 40.46%.

ACKNOWLEDGMENTS

This work is supported by the National Natural Science Foundation of China (52131102), to which the authors are most grateful.

REFERENCES

Arntsen, A (1996). "Disturbances, lift and drag forces due to the translation of a horizontal circular cylinder in stratified water," *Experiments in Fluids*, 21(5), 387-400.

Faltinsen, OM (2006). *Hydrodynamics of high-speed marine vehicles*, Cambridge University Press, 138-140.

Ferziger, JH, Milovan, P, and Anthony, L (1997). "Computational methods for fluid dynamics," *Physics Today*, 50(3), 80-84.

Grue, J, Friis, HA, Palm, E, and Rusås, PO (1997). "A method for computing unsteady fully nonlinear interfacial waves," *Journal of Fluid Mechanics*, 351, 223-252.

Gopala, VR, and Van Wachem, BG (2008). "Volume of fluid methods for immiscible-fluid and free-surface flows," *Chemical Engineering Journal*, 141(1-3), 204-221.

Landau, LD, Lifshitz, EM (1959). *Fluid mechanics*, Pergamon Press, 35-37.

Li, L, Zhao, B, and Sun, B (2023). "Surface Waves Induced by a Moving Submarine Model," *Journal of Marine Science and Application*, 22(1), 84-91.

Ma, W, Li, Y, Ding, Y, Duan, F, and Hu, K (2020). "Numerical investigation of internal wave and free surface wave induced by the DARPA Suboff moving in a strongly stratified fluid," *Ships and Offshore Structures*, 15(6), 587-604.

Mao, K, and Zhang, X (2013). "The general distribution characteristics of pycnocline of China Sea," *Marine Forecasts*, 30(6), 21-27.

Wang, C, Du, W, Li, G, et al. (2022). "Numerical simulation of influence of ocean internal waves on hydrodynamic characteristics of underwater vehicles," *Chinese Journal of Ship Research*, 17(3), 102–111.

Wei, G, Le, J, and Dai, S (2003). "Surface effects of internal wave generated by a moving source in a two-layer fluid of finite depth," *Applied Mathematics and Mechanics*, 24(9), 1025-1040.

Yeung, RW, and Nguyen, TC (1999). "Waves generated by a moving source in a two-layer ocean of finite depth," *Journal of Engineering Mathematics*, 35, 85-107.

Zhang, M, Liu, J, Mao, K, Li, Y, Zhang, X, and Shi, Y (2006). "The general distribution characteristics of thermocline of China Sea," *Mar. Forecast*, 23, 51-58.

Zhang, Z, zhang, H, Wang, Y, and Ma T (2022). "Numerical simulation of internal wave propagation in two-layer fluid under two water surface boundary conditions," *Hydro-Science and Engineering*, 2, 58-67.

Zhao, B, Wang, Z, Duan, W, Ertekin, RC, Hayatdavoodi, M, and Zhang, T (2020). "Experimental and numerical studies on internal solitary waves with a free surface," *Journal of Fluid Mechanics*, 899, A17.